Robust Thruster Fault Diagnosis : Application to the rendezvous phase of the Mars Sample Return mission

Robert Fonod, David Henry, Catherine Charbonnel, Eric Bornschlegl

Robust Thruster Fault Diagnosis : Application to the rendezvous phase of the Mars Sample Return mission

Robert Fonod, David Henry, Catherine Charbonnel and Eric Bornschlegl

Abstract This paper addresses robust fault diagnosis of the chaser's thrusters used for the rendezvous phase of the Mars Sample Return (MSR) mission. The MSR mission is a future exploration mission undertaken jointly by the National Aeronautics and Space Administration (NASA) and the European Space Agency (ESA). The goal is to return tangible samples from Mars atmosphere and ground to Earth for analysis. A residual-based scheme is proposed that is robust against the presence of unknown time-varying delays induced by the thruster modulator unit. The proposed fault diagnosis design is based on Eigenstructure Assignment (EA) and first-order Padé approximation. The resulted method is able to detect quickly any kind of thruster faults and to isolate them using a cross-correlation based test. Simulation results from the MSR "high-fidelity" industrial simulator, provided by Thales Alenia Space, demonstrate that the proposed method is able to detect and isolate some thruster faults in a reasonable time, despite of delays in the thruster modulator unit, inaccurate navigation unit, and spatial disturbances (i.e. J_2 gravitational perturbation, atmospheric drag, and solar radiation pressure).

Robert Fonod
IMS laboratory, University of Bordeaux 1, 351 cours de la libération, 33405 Talence, France
e-mail: robert.fonod@ims-bordeaux.fr

David Henry
IMS laboratory, University of Bordeaux 1, 351 cours de la libération, 33405 Talence, France
e-mail: david.henry@ims-bordeaux.fr

Catherine Charbonnel
Thales Alenia Space, 100 Boulevard du Midi, 06156 Cannes La Bocca, France
e-mail: catherine.charbonnel@thalesaleniaspace.com

Eric Bornschlegl
European Space Research and Technology Centre, Keplerlaan 1, 2200 AG Noordwijk, Netherlands
e-mail: eric.bornschlegl@esa.int

1 Introduction

Many space exploration missions require critical autonomous proximity operation. Mission safety is usually guaranteed through a hierarchical implementation of the fault diagnosis and fault tolerance with several levels of faults containments defined from local component/equipment up to global system, i.e. through various equipments (sensors like IMUs, thrusters, reaction wheels etc..) redundancy paths and ground intervention.

Classical Fault Detection Isolation and Recovery (FDIR) hierarchical implementation approach (see for instance [3, 15]) may be not sufficient in dynamics deviation in critical Space operations. This is specially the case for thruster faults during rendezvous and docking/capture proximity operations, and this could lead to mission loss. On-board robustness and fault tolerance/recovery shall prevail in the dynamics trajectory conditions.

The objective of this study is to develop an advanced model-based Fault Detection and Isolation (FDI) scheme able to diagnose thrusters' faults of the Mars Sample Return (MSR) chaser spacecraft, on-board/on-line and in time within the critical dynamics and operations constraints of the last terminal translation (last 20m) of the rendezvous/capture phase. As mission scenario undertaken, the chaser stays in the rendezvous/capture corridor, such that it is possible to anticipate the necessary recovery actions to successfully meet the capture phase, see Fig. 1 for an illustration.

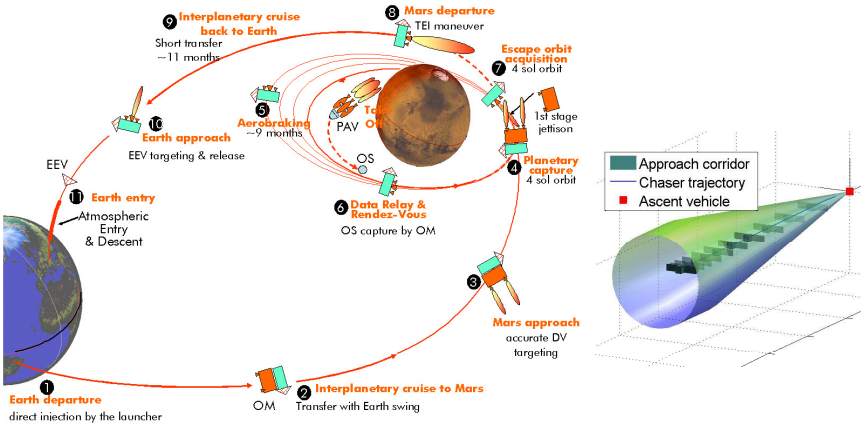

Fig. 1 Illustration of the rendezvous phase of the MSR mission

Numerous fault diagnosis methods are applicable to this problem [12, 13]. In fact, most of the model-based diagnostic techniques reported in the literature have the potential to be applied, see [2, 6, 9, 18] for good surveys. In recent years, some effective techniques of the fault detection and diagnosis for satellite attitude control

systems based on inertial wheels have been developed, see for instance the books [1, 10] and the references given therein. The problem of thrusters' faults is less considered in the literature. Among the contributions, one can refer to [5] where an Iterative Learning Observer (ILO) is designed to achieve estimation of time-varying thruster faults. The method proposed in [16, 17] is based on the so-called unknown input observer technique and is applied to the Mars Express mission. The work [11] addressed the problem of thrusters' faults diagnosis in the Microscope satellite and [7] considered the problem of faults affecting the micro-Newton colloidal thrust system of the LISA Pathfinder experiment. Both proposed FDI schemes are based on H_∞/H_- filters to generate residuals robust against spatial disturbances (i.e. J_2 disturbances, atmospheric drag and solar radiation), measurement noises and sensor misalignment phenomena, whilst guaranteeing fault sensitivity performances. Additionally, a Kalman-based projected observer scheme is considered in [7].

In this paper, the proposed FDI scheme consists of a residual generator that is robust against unknown time-varying delays induced by the thruster modulator unit and uncertainties on the thruster rise times. These uncertainties are transformed using Padé approximation to unknown inputs and decoupled by means of Eigenstructure Assignment (EA) technique. This detection scheme allows to detect quickly any kind of thruster faults. The isolation task is solved using a cross-correlation based test between the residual signal and the associated thruster open rate. For reduced computational burdens, the isolation test is based on a sliding time window. The key feature of the proposed method is the use of a judiciously chosen linear model for the design of the FDI scheme, i.e. a model that consists of a 6-order model taking into account both the rotational and linear translation of the spacecraft motions.

The paper is organized as follows: section 2 addresses some theoretical basements. The goal is to develop a robust FDI scheme for linear systems with unknown time-varying delays in the control input. It is shown that this problem can be solved using the unknown input decoupling approach by means of EA technique. Section 3 is devoted to the application of the proposed method to the problem of fault detection and isolation of the thrusters that equip the chaser spacecraft involved in the MSR mission.

2 Problem Description and the Theoretical Foundation of the Selected FDI Technique

Consider a continuous-time system given by

$$\begin{cases} \dot{\mathbf{x}}(t) = \mathbf{A}\mathbf{x}(t) + \mathbf{B}\mathbf{u}\big(t - \tau(t)\big) + \mathbf{E}_f\mathbf{f}(t) \\ \mathbf{y}(t) = \mathbf{C}\mathbf{x}(t) \end{cases} \tag{1}$$

where $\mathbf{x}(t) \in \mathbb{R}^n$ is the state vector, $\mathbf{u}(t) \in \mathbb{R}^{n_u}$ is the non-delayed system input vector, $\mathbf{y}(t) \in \mathbb{R}^{n_y}$ is the vector of the available measurements and $\mathbf{f}(t) \in \mathbb{R}^{n_f}$ is the fault vector. $\mathbf{A}$, $\mathbf{B}$, $\mathbf{C}$ and $\mathbf{E}_f$ are known matrices of appropriate dimensions. The

pair $(\mathbf{A},\mathbf{C})$ is assumed to be observable. The time-varying delay $\tau(t)$, induced by the electronic devices, is assumed to be unknown but upper bounded $\tau(t) \leq \bar{\tau}$.

Problem 1. Design a residual generator that is robust in the presence of uncertain time-varying delay $\tau(t)$.

In order to solve problem 1, a robust residual generator approach is presented in this paper. The aim is to model the influence of the uncertain time-varying delay as an unknown input. This will be done by using a first-order Padé approximation and introducing a new augmented state space description. Then, the unknown inputs are decoupled by means of EA technique.

2.1 Padé Approximation

The transfer function of the time delay is $H(s) = e^{-\tau(t)s}$. This transfer is irrational and it is necessary to substitute $e^{-\tau(t)s}$ with an approximation in form of a rational transfer function. The most common approximation is the Padé approximation

$$e^{-\tau(t)s} \doteq \frac{1 - k_1 s + k_2 s^2 + \ldots \pm k_n s^p}{1 + k_1 s + k_2 s^2 + \ldots + k_n s^p} \tag{2}$$

where p is the order of the approximation and the coefficients k_i are functions of p.

In this paper, a first-order Padé approximation of the time-varying delay $\tau(t)$ is used, when $k_1 = \frac{\tau(t)}{2}$ and $k_i = 0$, $i = 2,\ldots,p$, that is:

$$e^{-\tau(t)s} \doteq \frac{1 - \frac{\tau(t)}{2}s}{1 + \frac{\tau(t)}{2}s} \tag{3}$$

Considering all system inputs, the transfer function (3) is equivalent with the following state space representation

$$\begin{cases} \dot{\mathbf{x}}_d(t) = \mathbf{A}_d(t)\mathbf{x}_d(t) + \mathbf{B}_d\mathbf{u}(t) \\ \mathbf{u}(t-\tau(t)) = \mathbf{C}_d(t)\mathbf{x}_d(t) + \mathbf{D}_d\mathbf{u}(t) \end{cases} \tag{4}$$

where $\mathbf{x}_d(t) \in \mathbb{R}^{n_u}$ is the delayed state, $\mathbf{u}(t-\tau(t)) \in \mathbb{R}^{n_u}$ is the delayed input, and $\mathbf{A}_d(t) = -\frac{2}{\tau(t)}\mathbf{I}$, $\mathbf{B}_d = \mathbf{I}$, $\mathbf{C}_d(t) = \frac{4}{\tau(t)}\mathbf{I}$, $\mathbf{D}_d = -\mathbf{I}$ are matrices with appropriate dimension. Furthermore, using (1) and (4), and introducing a new augmented state vector of the form $\mathbf{z}^T(t) = \left[\mathbf{x}^T(t)\ \mathbf{x}_d^T(t)\right]$, we obtain:

$$\begin{cases} \dot{\mathbf{z}}(t) = \hat{\mathbf{A}}(t)\mathbf{z}(t) + \hat{\mathbf{B}}\mathbf{u}(t) + \hat{\mathbf{E}}_f\mathbf{f}(t) \\ \mathbf{y}(t) = \hat{\mathbf{C}}\mathbf{z}(t) \end{cases} \tag{5}$$

where

$$\hat{\mathbf{A}}(t) = \begin{bmatrix} \mathbf{A} & \mathbf{B}\mathbf{C}_d(t) \\ \mathbf{0} & \mathbf{A}_d(t) \end{bmatrix}, \hat{\mathbf{B}} = \begin{bmatrix} \mathbf{B}\mathbf{D}_d \\ \mathbf{B}_d \end{bmatrix}, \hat{\mathbf{C}} = \begin{bmatrix} \mathbf{C} & \mathbf{0} \end{bmatrix}, \hat{\mathbf{E}}_f = \begin{bmatrix} \mathbf{E}_f \\ \mathbf{0} \end{bmatrix}$$

It can be seen, that thanks to the chosen state-space representation (4), the uncertainty is present only in $\hat{\mathbf{A}}(t)$. The task is to decompose this matrix into the constant and time-varying part and to model the uncertainty as an unknown input.

2.2 Expressing the Uncertainty as an Unknown Input

Problem 2. Decompose the matrix $\hat{\mathbf{A}}(t)$ in two parts:

$$\hat{\mathbf{A}}(t) = \hat{\mathbf{A}}_0 + \Delta\hat{\mathbf{A}}(t) \tag{6}$$

where $\hat{\mathbf{A}}_0$ is a constant matrix and $\Delta\hat{\mathbf{A}}(t)$ is the time-varying part of $\hat{\mathbf{A}}(t)$.

Consider, that $\tau(t)$ can be expressed as

$$\tau(t) = \tau_0 + \delta(t) \ : \ |\delta(t)| \leq \bar{\delta} \tag{7}$$

where τ_0 is the nominal delay, $\delta(t)$ is the variation around τ_0, and $\bar{\delta}$ is the upper bound of the variation part.

Proposition 1. *Let $a \in \mathbb{R}$ and $b \in \mathbb{R}$ be two real scalars, where $a \neq 0$ and $a+b \neq 0$, then*

$$(a+b)^{-1} = a^{-1} - a^{-1}\frac{b}{a+b} \tag{8}$$

Proof. Using some basic arithmetic operations, it can be shown, that (8) holds. □

Therefore, using proposition 1, we can write

$$\frac{1}{\tau(t)} = \big(\tau_0 + \delta(t)\big)^{-1} = \frac{1}{\tau_0} - \frac{1}{\tau_0}\delta^*(t) \tag{9}$$

where $\delta^*(t) = \frac{\delta(t)}{\tau_0+\delta(t)}$. Problem 2 is solved using (9), that is

$$\hat{\mathbf{A}}_0 = \begin{bmatrix} \mathbf{A} & \mathbf{B}\mathbf{C}_d^{\tau_0} \\ \mathbf{0} & \mathbf{A}_d^{\tau_0} \end{bmatrix}, \quad \Delta\hat{\mathbf{A}}(t) = \begin{bmatrix} \mathbf{0} & -\mathbf{B}\mathbf{C}_d^{\tau_0} \\ \mathbf{0} & -\mathbf{A}_d^{\tau_0} \end{bmatrix}\delta^*(t) \tag{10}$$

where $\mathbf{A}_d^{\tau_0} = -\frac{2}{\tau_0}\mathbf{I}$ and $\mathbf{C}_d^{\tau_0} = \frac{4}{\tau_0}\mathbf{I}$.

The time-varying part $\Delta\hat{\mathbf{A}}(t)$ can be expressed as an unknown input $\mathbf{d}(t)$, entering the augmented dynamics (5) through $\hat{\mathbf{E}}_d$, by:

$$\Delta\hat{\mathbf{A}}(t)\mathbf{z}(t) = \begin{bmatrix} \mathbf{0} & -\mathbf{B}\mathbf{C}_d^{\tau_0} \\ \mathbf{0} & -\mathbf{A}_d^{\tau_0} \end{bmatrix}\delta^*(t)\mathbf{z}(t) = \hat{\mathbf{E}}_d\mathbf{d}(t) \tag{11}$$

where

$$\hat{\mathbf{E}}_d = \begin{bmatrix} -\mathbf{B}\mathbf{C}_d^{\tau_0} \\ -\mathbf{A}_d^{\tau_0} \end{bmatrix}, \quad \mathbf{d}(t) = \delta^*(t)\mathbf{x}_d(t) \tag{12}$$

Now, taking the above notation into account, the design model is expressed in terms of unknown inputs as

$$\begin{cases} \dot{\mathbf{z}}(t) = \hat{\mathbf{A}}_0\mathbf{z}(t) + \hat{\mathbf{B}}\mathbf{u}(t) + \hat{\mathbf{E}}_f\mathbf{f}(t) + \hat{\mathbf{E}}_d\mathbf{d}(t) \\ \mathbf{y}(t) = \hat{\mathbf{C}}\mathbf{z}(t) \end{cases} \tag{13}$$

This model is the augmented representation of the original system (1), which takes into account uncertainties caused by electronic-induced delays represented as an additional unknown input $\mathbf{d}(t)$.

2.3 Residual Generator Design Using Eigenstructure Assignment

In order to solve problem 1, we define the following structure of the residual generator based on full-order observer (see e.g. [4, 14])

$$\begin{cases} \dot{\mathbf{z}}_e(t) = (\hat{\mathbf{A}}_0 - \mathbf{L}\hat{\mathbf{C}})\mathbf{z}_e(t) + \hat{\mathbf{B}}\mathbf{u}(t) + \mathbf{L}\mathbf{y}(t) \\ \mathbf{r}(t) = \mathbf{W}\big(\mathbf{y}(t) - \hat{\mathbf{C}}\mathbf{z}_e(t)\big) \end{cases} \tag{14}$$

where $\mathbf{r} \in \mathbb{R}^{n_p}$ is the residual vector and $\mathbf{z}_e(t) \in \mathbb{R}^{n+n_u}$ is the augmented state estimation. The matrix $\mathbf{W} \in \mathbb{R}^{n_p \times n_y}$ is the residual weighting matrix.

The Laplace transformed residual response to faults and unknown inputs is

$$\mathbf{r}(s) = \mathbf{G}_{rf}(s)\mathbf{f}(s) + \mathbf{G}_{rd}(s)\mathbf{d}(s) \tag{15}$$

where

$$\mathbf{G}_{rf}(s) = \mathbf{W}\hat{\mathbf{C}}(s\mathbf{I} - \hat{\mathbf{A}}_0 + \mathbf{L}\hat{\mathbf{C}})^{-1}\hat{\mathbf{E}}_f \tag{16}$$

$$\mathbf{G}_{rd}(s) = \mathbf{W}\hat{\mathbf{C}}(s\mathbf{I} - \hat{\mathbf{A}}_0 + \mathbf{L}\hat{\mathbf{C}})^{-1}\hat{\mathbf{E}}_d \tag{17}$$

Once $\hat{\mathbf{E}}_d$ is known, the remaining problem is to find the matrices $\mathbf{L}$ and $\mathbf{W}$ to satisfy $\mathbf{G}_{rd}(s) = \mathbf{0}$. The assignment of the observer's eigenvectors and eigenvalues is a direct way to solve this design problem.

2.3.1 Unknown Input Decoupling by Assigning Left Eigenvectors

Lemma 1. *The transfer function $\mathbf{G}_{rd}(s)$ can be expanded in terms of the eigenstructure as*

$$\mathbf{G}_{rd}(s) = \mathbf{H}(s\mathbf{I} - \hat{\mathbf{A}}_c)^{-1}\hat{\mathbf{E}}_d = \sum_{i=1}^{n} \frac{\mathbf{F}_i}{s - \lambda_i} = \sum_{i=1}^{n} \frac{\mathbf{H}\mathbf{v}_i\mathbf{l}_i^T\hat{\mathbf{E}}_d}{s - \lambda_i} \tag{18}$$

where $\mathbf{H} = \mathbf{W}\hat{\mathbf{C}}$, $\mathbf{F}_i = \mathbf{H}\mathbf{v}_i\mathbf{l}_i^T\hat{\mathbf{E}}_d$, $\mathbf{v}_i$ *and* $\mathbf{l}_i^T$ *are the right and left eigenvectors of* $\hat{\mathbf{A}}_c = \hat{\mathbf{A}}_0 - \mathbf{L}\hat{\mathbf{C}}$ *associated with eigenvalue* λ_i.

Lemma 2. *It is well known that, a given left eigenvector* $\mathbf{l}_i^T$ *of* $\hat{\mathbf{A}}_c$ *is always orthogonal to the right eigenvectors* $\mathbf{v}_j$ *corresponding to the remaining* $(n-1)$ *eigenvalues* λ_j *of* $\hat{\mathbf{A}}_c$, *where* $\lambda_i \neq \lambda_j$.

Theorem 1 (Chen and Patton, 1999). *If* $\mathbf{W}\hat{\mathbf{C}}\hat{\mathbf{E}}_d = \mathbf{0}$ *and all rows of the matrix* $\mathbf{H}$ *are left eigenvectors of* $\hat{\mathbf{A}}_c$ *corresponding to* n_p *eigenvalues of* $\hat{\mathbf{A}}_c$, *then* $\mathbf{G}_{rd}(s) = \mathbf{0}$.

Proof. If the rows of $\mathbf{H}$ are n_p left eigenvectors $(\mathbf{l}_i, i = 1,\ldots,n_p)$ of $\hat{\mathbf{A}}_c$, i.e.

$$\mathbf{H} = \begin{bmatrix} \mathbf{l}_1 & \mathbf{l}_2 & \ldots & \mathbf{l}_{n_p} \end{bmatrix}^T \tag{19}$$

then $\mathbf{H}\mathbf{v}_i = \mathbf{0}$ and $\mathbf{F}_i = \mathbf{0}$ for $i = n_p+1,\ldots,n$. If further we have $\mathbf{W}\hat{\mathbf{C}}\hat{\mathbf{E}}_d = \mathbf{H}\hat{\mathbf{E}}_d = \mathbf{0}$, i.e. $\mathbf{l}_i^T\hat{\mathbf{E}}_d = \mathbf{0}$ and $\mathbf{F}_i = \mathbf{0}$ for $i = 1,2,\ldots,n_p$, thus $\mathbf{G}_{rd}(s) = \mathbf{0}$. □

The first step for the design of an unknown input decoupled residual generator (14) is to compute the weighting matrix $\mathbf{W}$ which must satisfy the following necessary condition [4]

$$\mathbf{W}\hat{\mathbf{C}}\hat{\mathbf{E}}_d = \mathbf{H}\hat{\mathbf{E}}_d = \mathbf{0} \tag{20}$$

The necessary and sufficient condition for solution (20) to exist is $\text{rank}(\hat{\mathbf{C}}\hat{\mathbf{E}}_d) < n_y$. If $\hat{\mathbf{C}}\hat{\mathbf{E}}_d = \mathbf{0}$, any weighting matrix can satisfy this necessary condition. A general solution is

$$\mathbf{W} = \mathbf{W}_1(\mathbf{I} - \hat{\mathbf{C}}\hat{\mathbf{E}}_d(\hat{\mathbf{C}}\hat{\mathbf{E}}_d)^+) \tag{21}$$

where $\mathbf{W}_1 \in \mathbb{R}^{n_p \times n_y}$ is an arbitrary matrix and $(\hat{\mathbf{C}}\hat{\mathbf{E}}_d)^+$ is the pseudo-inverse of $(\hat{\mathbf{C}}\hat{\mathbf{E}}_d)$, defined as $(\hat{\mathbf{C}}\hat{\mathbf{E}}_d)^+ = ((\hat{\mathbf{C}}\hat{\mathbf{E}}_d)^T(\hat{\mathbf{C}}\hat{\mathbf{E}}_d))^{-1}(\hat{\mathbf{C}}\hat{\mathbf{E}}_d)^T$.

The second step is to determine the eigenstructure of the observer. The rows of $\mathbf{H}$ must be the n_p left eigenvectors of $\hat{\mathbf{A}}_c$. The remaining $n-n_p$ left eigenvectors can be chosen without restraint. For the given (stable) eigenvalue spectrum $\Lambda(\hat{\mathbf{A}}_c) = \{\lambda_i, i = 1,\ldots,n\}$, the following relation holds

$$\mathbf{l}_i^T(\lambda_i\mathbf{I} - \hat{\mathbf{A}}_0) = -\mathbf{l}_i^T\mathbf{L}\hat{\mathbf{C}} = -\mathbf{m}_i^T\hat{\mathbf{C}}, \quad i = 1,\ldots,n \tag{22}$$

where $\mathbf{m}_i^T = \mathbf{l}_i^T\mathbf{L}$. The assignability condition says, that for each λ_i, the corresponding left eigenvector $\mathbf{l}_i^T$ should lie in the column subspace spanned by $\{\hat{\mathbf{C}}(\lambda_i\mathbf{I} - \hat{\mathbf{A}}_0)^{-1}\}$, i.e. a vector $\mathbf{m}_i$ exists such that

$$\mathbf{l}_i^T = \mathbf{m}_i^T\mathbf{K}_i, \qquad i = 1,\ldots,n_p \tag{23}$$

where $\mathbf{K}_i = -\hat{\mathbf{C}}(\lambda_i\mathbf{I} - \hat{\mathbf{A}}_0)^{-1}$, $i = 1,\ldots,n_p$. The projection of $\mathbf{l}_i$ in the subspace $\text{span}\{\mathbf{K}_i\}$ is denoted by:

$$\mathbf{l}_i^{\circ T} = \mathbf{m}_i^{\circ T}\mathbf{K}_i, \qquad i = 1,\ldots,n_p \tag{24}$$

where $\mathbf{m}_i^{\circ T} = \mathbf{l}_i^T \mathbf{K}_i^T (\mathbf{K}_i \mathbf{K}_i^T)^{-1}, i = 1, \ldots, n_p$. If $\mathbf{l}_i^T = \mathbf{l}_i^{\circ T}$, $\mathbf{l}_i^T$ is in span$\{\mathbf{K}_i\}$ and is assignable. Otherwise, an approximative procedure must be considered in order to replace $\mathbf{l}_i^T$ by it's projection $\mathbf{l}_i^{\circ T}$.

The remaining $n - n_p$ eigenvalues and corresponding eigenvectors can be chosen freely from the assignable subspace and assigned using some EA technique, e.g. using singular value decomposition (SVD). Then, the observer matrix $\mathbf{L}$ can be computed as follows

$$\mathbf{L} = \mathbf{P}^{-1}\mathbf{M} \tag{25}$$

where

$$\mathbf{M} = \begin{bmatrix} \mathbf{m}_1^\circ & \ldots & \mathbf{m}_{n_p}^\circ & \mathbf{m}_{n_{p+1}} & \ldots & \mathbf{m}_n \end{bmatrix}^T$$
$$\mathbf{P} = \begin{bmatrix} \mathbf{l}_1^\circ & \ldots & \mathbf{l}_{n_p}^\circ & \mathbf{l}_{n_{p+1}} & \ldots & \mathbf{l}_n \end{bmatrix}^T$$

It is obvious, that the first n_p eigenvalues corresponding to the required eigenvectors $\mathbf{l}_i^T, i = 1, \ldots, n_p$ must be real because all these eigenvectors are real-valued.

Remark 1. The remaining design freedom, after unknown input de-coupling, can be used to optimize other performance indices such as fault sensitivity.

3 Application to the MSR Mission

The robust fault detection scheme presented in the above section is now considered for the detection and isolation of the faults affecting the chaser's thrusters unit.

3.1 Modeling the Chaser Dynamics During the Rendezvous Phase

In the interest of brevity, from [8, 19, 20, 21] we only consider the modeling of the relative position of two spacecrafts on a circular orbit around the planet.

The motion of the chaser is derived from the 2nd Newton law. To proceed, let a, m, $\mathscr{G}$ and m_M denote the orbit of the target, the mass of the chaser, the gravitational constant and the mass of the planet Mars. Then, the orbit of the rendezvous being circular, the velocity of any object (e.g. the chaser and the target) is given by the relation $\sqrt{\frac{\mu}{a}}$ where $\mu = \mathscr{G}.m_M$. Let $\mathscr{R}_l : (O_{tgt}, \overrightarrow{X_l}, \overrightarrow{Y_l}, \overrightarrow{Z_l})$ be the frame attached to the target and oriented as shown in Fig. 2. Because the linear velocity of the target is given by the relation $a\dot{\theta}$ in the inertial frame $\mathscr{R}_i : (O_M, \overrightarrow{X_i}, \overrightarrow{Y_i}, \overrightarrow{Y_i})$ (see Fig. 2), it follows:

$$a.\dot{\theta} = \sqrt{\frac{\mu}{a}} \Rightarrow n = \sqrt{\frac{\mu}{a^3}} \tag{26}$$

During the rendezvous phase, it is assumed that the chaser motion is due to the four forces: Mars attraction force, centripetal force, Coriolis force and forces due to the thrusters (F_x, F_y, F_z). Then, from the 2nd Newton law, it follows

$$\begin{aligned}
\ddot{x} &= n^2 x + 2n\dot{y} - \frac{\mu}{\left((a+x)^2+y^2+z^2\right)^{3/2}}(a+x) + \frac{F_x}{m} \\
\ddot{y} &= n^2 y - 2n\dot{x} - \frac{\mu}{\left((a+x)^2+y^2+z^2\right)^{3/2}} y + \frac{F_y}{m} \\
\ddot{z} &= -\frac{\mu}{\left((a+x)^2+y^2+z^2\right)^{3/2}} z + \frac{F_z}{m}
\end{aligned} \tag{27}$$

where x ,y, z denote the three dimensional position of the chaser (assumed to be a punctual mass) in $\mathscr{R}_l$.

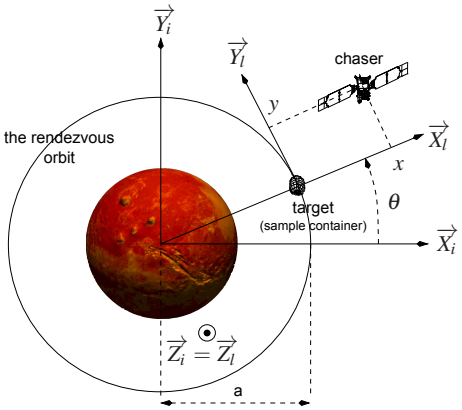

Fig. 2 The Mars rendezvous orbit and the associated frames

Because the distance between the target and the chaser is smaller than the orbit a, it is possible to derive the so called Hill-Clohessy-Wiltshire (HCW) equations from (27) by means of a first order approximation. This boils down to a linear six order state space model with the input vector $\mathbf{u}(t) = (F_x\, F_y\, F_z)^T$, output vector $\mathbf{y}(t) = (x\, y\, z)$ and state vector $\mathbf{x}(t) = (x\, y\, z\, \dot{x}\, \dot{y}\, \dot{z})^T$, i.e. from (27) it follows

$$\begin{cases}
\dot{\mathbf{x}}(t) = \mathbf{A}\mathbf{x}(t) + \mathbf{B}\mathbf{R}\left(\hat{Q}_{tgt}(t), \hat{Q}_{chs}(t)\right)\overline{\mathbf{M}}\mathbf{u}_{thr}(t) + \mathbf{E}_w\mathbf{w}(t) \\
\mathbf{y}(t) = \mathbf{C}\mathbf{x}(t) \\
\mathbf{y}_m(t) = -\mathbf{y}(t) + \mathbf{v}(t)
\end{cases} \tag{28}$$

where

$$\mathbf{A} = \begin{bmatrix}
0 & 0 & 0 & 1 & 0 & 0 \\
0 & 0 & 0 & 0 & 1 & 0 \\
0 & 0 & 0 & 0 & 0 & 1 \\
0 & 0 & 0 & 0 & 0 & 2n \\
0 & -n^2 & 0 & 0 & 0 & 0 \\
0 & 0 & 3n^2 & -2n & 0 & 0
\end{bmatrix}, \mathbf{B} = \mathbf{E}_w = \frac{1}{m}\begin{bmatrix}
0 & 0 & 0 \\
0 & 0 & 0 \\
0 & 0 & 0 \\
1 & 0 & 0 \\
0 & 1 & 0 \\
0 & 0 & 1
\end{bmatrix}, \mathbf{C} = \begin{bmatrix}
1 & 0 & 0 & 0 & 0 & 0 \\
0 & 1 & 0 & 0 & 0 & 0 \\
0 & 0 & 1 & 0 & 0 & 0
\end{bmatrix} \tag{29}$$

Further, $\hat{Q}_{tgt}(t) \in \mathbb{R}^4$ and $\hat{Q}_{chs}(t) \in \mathbb{R}^4$ denote the attitude's quaternion of the target and the chaser, respectively. These quaternions are estimates from the navigation module (NAV). $\overline{\mathbf{M}} \in \mathbb{R}^{3\times 8}$ refers to the thrusters' configuration (direction) matrix, $\mathbf{u}_{thr}(t) = (u_{thr_1}(t), ..., u_{thr_8}(t))^T$, $0 \leq u_{thr_i}(t) \leq 1$, $i = 1, ..., 8$ are the thruster inputs, $\mathbf{y}_m(t) \in \mathbb{R}^3$ is the three-dimensional position measured by a LIDAR unit that is corrupted by the measurement noise $\mathbf{v}(t) \in \mathbb{R}^3$ and $\mathbf{w}(t) \in \mathbb{R}^3$ refers to spatial disturbances. The quaternions dependent rotation matrix $\mathbf{R}(.)$ performs the projection of the three-dimensional thrust forces (due to the eight thrusters that equip the chaser) from the chaser's frame on to the target frame $\mathscr{R}_l$. The numerical values of the parameters are not shown for reasons of confidentiality.

The considered thruster faults can be modeled in a multiplicative manner according to (the index "f" is used to outline the faulty case)

$$\mathbf{u}_{thr}^f(t) = \big(\mathbf{I}_8 - \Psi(t)\big)\mathbf{u}_{thr}(t), \quad \Psi(t) = diag\big(\psi_1(t), \ldots, \psi_8(t)\big) \tag{30}$$

where $0 \leq \psi_i(t) \leq 1$, $i = 1, ..., 8$ are unknown. $\Psi(t)$ models thruster faults, e.g. a locked-in-placed fault can be modeled by $\Psi_i(t) = 1 - \frac{c}{u_{thr_i}(t)}$ where c denotes a constant value (the particular values $c = \{0, 1\}$ allows to consider closed/open faults) whereas a fix value of $\Psi_i(t)$ models a loss of efficiency of the i^{th} thruster.

During the rendezvous phase, the thruster management algorithm operates in the 6DOF mode. It means, that both commanded torque and force are achieved by thrusters only and thus the thruster faults affect the attitude of the chaser spacecraft.

Taking into account some unknown but bounded delays induced by the electronic devices, and uncertainties on the thruster rise times due to the thruster modulator unit that is modeled here as an unknown time-varying delay $\tau(t) = \tau_0 + \delta(t)$ with a (constant) nominal delay τ_0 and upper bounded variation part $|\delta(t)| \leq \bar{\delta}$. The motion of the chaser during the rendezvous can be modeled in both fault free (i.e. $\Psi(t) = 0$) and faulty (i.e. $\Psi(t) \neq 0$) situations according to

$$\begin{cases} \dot{\mathbf{x}}(t) = \mathbf{A}\mathbf{x}(t) + \mathbf{B}\mathbf{R}\big(\hat{Q}_{tgt}(t), \hat{Q}_{chs}(t)\big)\overline{\mathbf{M}}\big(\mathbf{I} - \Psi(t)\big)\mathbf{u}_{thr}\big(t - \tau(t)\big) + \mathbf{E}_w\mathbf{w}(t) \\ \mathbf{y}(t) = \mathbf{C}\mathbf{x}(t) = -\mathbf{y}_m(t) + \mathbf{v}(t) \end{cases} \tag{31}$$

Now considering $\mathbf{R}(\hat{Q}_{tgt}(t), \hat{Q}_{chs}(t))\overline{\mathbf{M}}\mathbf{u}_{thr}(t)$ as the input vector $\mathbf{u}(t)$, and approximating the fault model $-\mathbf{R}(\hat{Q}_{tgt}(t), \hat{Q}_{chs}(t))\overline{\mathbf{M}}\Psi(t)\mathbf{u}_{thr}(t)$ in terms of additive faults $\mathbf{f}(t) \in \mathbb{R}^3$ acting on the state via a constant distribution matrix $\mathbf{E}_f$ (then $\mathbf{E}_f = \mathbf{B}$), it follows that the overall model of the relative dynamics that takes into account both, the attitude $Q_{chs}(t)$, and the relative position $(x\ y\ z)$ of the chaser and the target can be written in the form (1).

3.2 Design of the FDI Scheme

3.2.1 Design of the Residual Generator

To design a residual generator $\mathbf{r}(t)$, the above derived model (31) is used. It is considered that $\mathbf{y}(t) = -\mathbf{y}_m(t)$. The sampling period T_s of the NAV is $0.1s$ and a reasonable value of the nominal time delay was determined to be exactly one sampling period for the input vector $\mathbf{u}(t)$. By using Padé approximation of the time delay $\tau(t)$, the uncertainty caused by the unknown time-varying parameter $\delta(t)$, introduced in (7), has been modeled as an unknown input $\mathbf{d}(t)$ entering the augmented state space dynamic (13) through the matrix $\hat{\mathbf{E}}_d$ computed as in (12), with $\tau_0 = 0.1$. Following the discussion in section 2.3.1, the residual weighting matrix was determined to be $\mathbf{W} = \mathbf{I}_3$, thus the dimension of the resulting residual is $n_p = 3$, i.e. $\mathbf{r}(t) = (r_1(t), r_2(t), r_3(t))^T$. All the assigned eigenvalues were chosen to be close to -0.5. Finally, the residual generator (14) is converted to discrete-time ($t = kT_s$) using a Tustin approximation and implemented within the nonlinear simulator of the MSR mission.

Remark 2. Since the spatial disturbances $\mathbf{w}(t)$ have the same directional properties as the faults, i.e. $\mathbf{E}_w = \mathbf{E}_f$, the residual signal $\mathbf{r}(t)$ cannot be decoupled from $\mathbf{w}(t)$.

3.2.2 Decision Test and the Isolation Strategy

To make a decision about the fault presence, a simple threshold-based decision test is applied to the residual norm $||\mathbf{r}(k)||_2$ as follows:

$$\begin{array}{ll} ||\mathbf{r}(k)||_2 < J_T; & \text{fault-free} \\ ||\mathbf{r}(k)||_2 \geq J_T; & \text{fault declared} \end{array} \tag{32}$$

where J_T is a fixed threshold and $||\cdot||$ denote the Euclidean vector norm.

The proposed isolation strategy is based on the following cross-correlation criterion between the j^{th} residual signal r_j and the associated controlled thrusters open rate u_{thr_i}, i.e.:

$$\sigma_j(k) = \arg\min_i \Big| \frac{1}{N} \sum_{l=k-N}^{k} r_j(k) u_{thr_i}(l) \Big|, \; i = 1...8, \; j \in \{1,2,3\}, \forall k \in \mathbb{Z}^+ \tag{33}$$

This cross-correlation function is a statistical quantity that tries to find the associated thruster index that has the smallest impact on the resulting residual signal. For real-time reason, this criterion is computed on a N-length sliding-window. The resulting index $\sigma_j(k) \in \{1,2,\ldots,8\}$ refers to the identified faulty thruster, using the j^{th} residual signal. The decision about the identified faulty thruster can be considered in three different ways, i.e. $\sigma(k)$ is computed:

1. as the smallest cross-correlation among all the residuals;

2. using only one residual signal $r_j(k)$, $j \in \{1,2,3\}$, e.g. the first $\sigma(k) = \sigma_1(k)$;
3. using a voting scheme where, for all residuals $r_j(k), j = 1,2,3$ a $\sigma_j(k)$ is computed separately, and a majority voting rule is implemented, i.e. the resulting index by the most $\sigma_j(k)$ is the identified faulty thruster.

A key feature of these isolation methods is that they are static and then, have a low computational burdens.

To make a final decision about the identified thruster index a *confirmation window* $N_c > 1$ is considered, i.e. the identified index is confirmed at time instant k, if:

$$\sigma(k) = \sigma(k-1) = \ldots = \sigma(k-N_s+1) \tag{34}$$

The whole FDI strategy works as follows: as soon as the fault is declared by the decision test (32), the above described isolation strategy is executed.

Remark 3. It is obvious, that if the i^{th} thruster is not used by the thruster management unit, i.e. $u_{thr_i} = 0$, the minimum cross-correlation will result in $\sigma(k) = i$. This fact must be taken into account, and the associated thruster rates below some predefined (small) threshold shall not be taken into account by the isolation strategy.

Remark 4. With the case of a number of thrusters greater than the DOF, some thruster faults evolve in the same residual sub-space, therefore using sub-space isolation approach, a full coverage of the isolation problematic cannot be guaranteed.

3.3 Simulation Results

As mentioned, the navigation unit is not considered to deliver "perfect" measurements. Due to this fact, the quaternion estimates and the LIDAR signal are additionally corrupted by noise that we modeled (according to the industrial specifications) as an uniform distributed noise. We consider delays between the navigation module and the control block, delays induced by the thruster modulator unit and spatial disturbances. The considered disturbances $\mathbf{w}(t)$ are solar radiations, J_2 gravitational perturbation and atmospheric drag. The simulated faults correspond to a single thruster opening at 100% during the last 20m of the rendezvous. Analysis of different fault scenarios are subject of the future research. The isolation strategy is computed according to (33) using the majority voting rule. The window length N_c for fault confirmation is taken as 10 sampling instants. Note that the *remark 3*, stated in section 3.2.2, was not considered in this simulation study.

Fig.3 illustrate the behavior of $\|r(t)\|_2$, the decision test, confirmation window (green area) and the isolation criteria $\sigma(k)$, for some faulty situations. For each simulation, the fault occurs at $t = 1200s$ and is maintained one minute.

As it can be seen from the figures, all thruster faults are successfully detected and isolated by the FDI unit with a reasonable detection and isolation time (see Table 1). Note that such a strategy succeeds since both the rotational $\left(Q_{chs}(t)\right)$ and linear

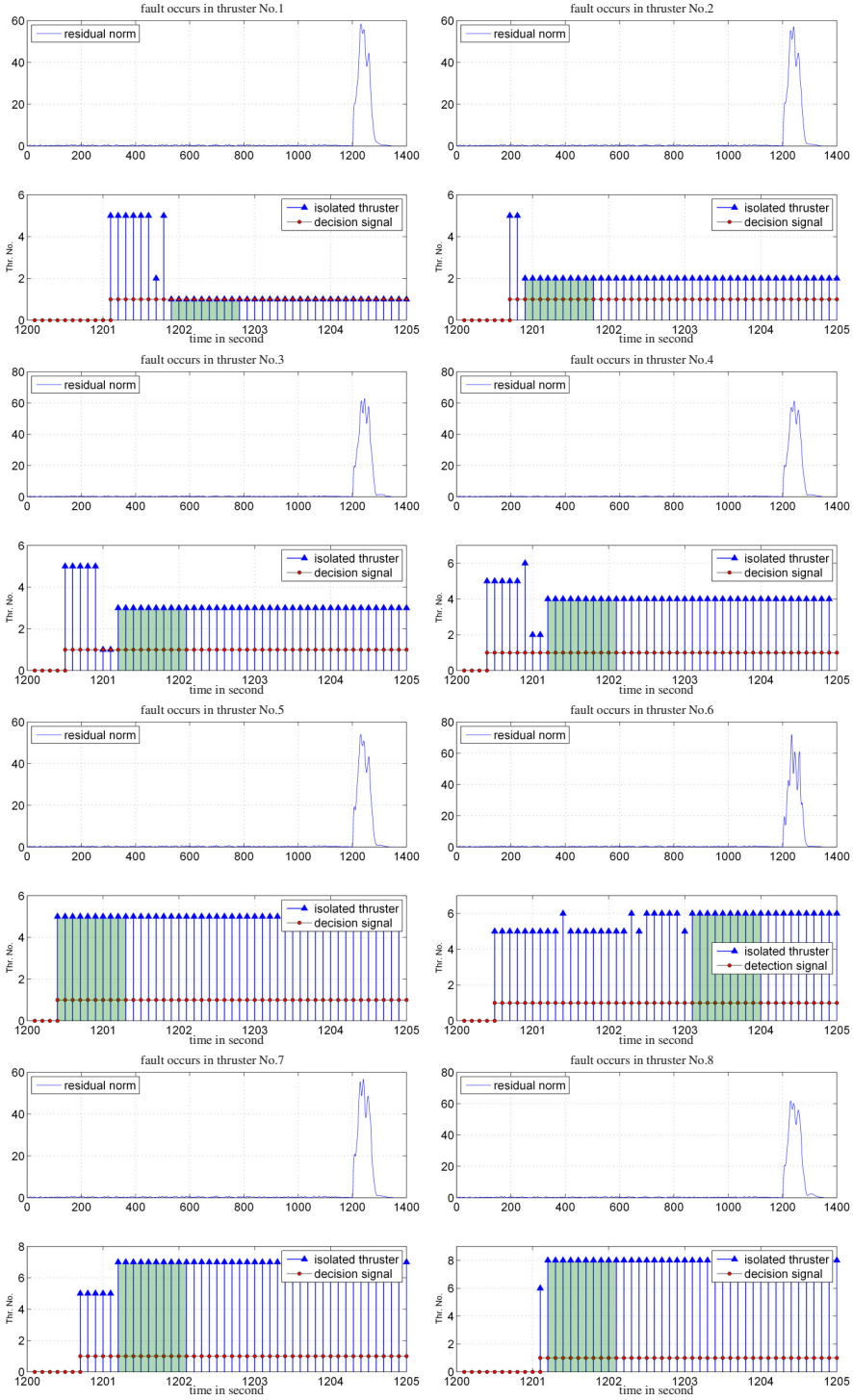

Fig. 3 Behaviour of the residual norm $\|r(k)\|_2$, isolation criteria $\sigma(k)$, decision signal and confirmation window for some faulty situations

translation $\left(\mathbf{x}(t)\right)$ of the chaser motions have been considered. Thus, the effects that faults have on both the chaser attitude and translation motion, are taken into account.

Table 1 Detection and isolation times in seconds

Thruster No.	**1**	**2**	**3**	**4**	**5**	**6**	**7**	**8**
Detection time	1.1s	0.7s	0.5s	0.4s	0.4s	0.5s	0.7s	1.1s
Isolation time	2.8s	1.8s	2.1s	2.1s	1.3s	4.0s	2.1s	2.1s

4 Concluding Remarks

This paper has proposed an EA-based fault diagnosis approach to detect and isolate thruster faults subject to time-varying delays induced by the thruster modulator unit. The resulted residual generator is robust against the uncertain time variations (approximated in terms of unknown inputs) around the nominal delay. The key feature of the proposed method is the use of a judiciously chosen linear model for the design of the residual generator, i.e. a model that takes into account both the rotational and translation dynamics of the spacecraft. This allows to propose a fault diagnosis solution with reduced computational burdens, which is a prior condition for an on-board implementation. Nonlinear simulations from the "high-fidelity" industrial simulator show that despite the presence of measurement noises, delays in the thruster modulator unit and spatial disturbances, the faults are successfully detected and isolated in a reasonable time.

Acknowledgements This research work was supported by the European Space Agency (ESA) and Thales Alenia Space in the frame of the ESA Networking/Partnering Initiative (NPI) Program.

References

1. Azarnoush, H. Fault Diagnosis in Spacecraft Attitude Control System: A Model-Based Approach. LAP LAMBERT Academic Publishing (2010)
2. Blanke, M., Kinnaert, M., Lunze, J., Staroswiecki, M.: Diagnosis and fault tolerant control. Springer, New York (2003)
3. Bornschleg, E.: FDIR requirements and rational - esa r&d activities overview for GNC and software. In: *CCT CNES*. Toulouse, France (2008)
4. Chen J., Patton, R.: Robust model-based fault diagnosis for dynamic systems. Kluwer Academic Publishers (1999)
5. Chen, W. Saif, M.: Observer-based fault diagnosis of satellite systems subject to time-varying thruster faults. *Journal of dynamic systems, measurement and control, Tr. of the ASME*, vol. 129, no. 3, pp. 352–356. (2007)

6. Ding, S.: Model-based Fault Diagnosis Techniques - Design schemes, Algorithms and Tools. Springer, New York (2008)
7. Falcoz, A., Boquet, F., Flandin, G.: Robust H_∞/H_- thruster failure detection and isolation with application to the LISA Pathfinder spacecraft. In: *AIAA Guidance, Navigation, and Control Conference*, (Toronto, Ontario), AIAA (2010)
8. Irvin, D.J.: A study of linear vs. nonlinear control techniques for the reconfiguration of satellite formations. PhD thesis, Air Force Institute of Technology (2001)
9. Isermann, R.: Model-based fault detection and diagnosis - status and applications. *Annual Reviews in Control*, vol. 29, pp. 71–85 (2005)
10. Hao, H., Sun, Z., Zhang, Y.: Fault Diagnosis on Satellite Attitude Control with Dynamic Neural Network. Lecture Notes in Computer Science. Springer, Berlin/Heidelberg (2004)
11. Henry, D. Fault diagnosis of the MICROSCOPE satellite actuators using H_∞/H_- filters. *AIAA Journal of Guidance, Control, and Dynamics*, vol. 31, no. 3, pp. 699–711. (2008)
12. Henry, D.: A norm-based point of view for fault diagnosis: Application to aerospace missions. *Automatic Control in Aerospace*, vol. 4, no. 1, p. online journal (2011)
13. Henry, D., Simani, S., Patton, R.: Fault Detection and Diagnosis for Aeronautic and Aerospace Missions in Fault Tolerant Flight Control: A Benchmark Challenge. Springer (2010)
14. Krokavec, D.: Residual generators design using eigenstructure assignment. In: *AT&P Journal Plus*, vol. 12, no. 2, pp. 72-74. (2007)
15. Olive, X.: FDI(R) for satellite at Thales Alenia Space: How to deal with high availability and robustness in space domain?. In: *Conference on Control and Fault-Tolerant Systems (SysTol'10)*, pp. 837–842. Nice, France (2010)
16. Patton, R., Uppal, F., Simani, S.,Polle, B.: Reliable fault diagnosis scheme for a spacecraft attitude control system. In: *Proc. IMechE. Part 0: Journal of Risk and Reliability*, vol. 222, pp. 139–152. (2008)
17. Patton, R., Uppal, F., Simani, S.,Polle, B.: Robust FDI applied to thruster faults of a satellite system. *Control Engineering Practice*, vol. 18, no. 9, pp. 1093–1109. (2010)
18. Venkatasubramanian, V., Rengaswamy, R., Yin, K., Kavuri, S. A review of process fault detection and diagnosis. part 1: Quantitative model-based methods. *Computer and Chemical Engineering*, vol. 27, no. 3, pp. 293–311. (2003)
19. Wertz, J.R., Larson, W.J.: Space Mission Analysis and Design (Third Edition). Springer, New York (1999)
20. Wied, B.: *Space vehicle dynamics and control*. American Institute of Aeronautics and Astronautics, Reston, VA (1998)
21. Wisniewski, R.: Lecture Notes on Modelling of a Spacecraft. Aldeling for Proceskontrol, Aalborg Universitet (2000)
22. Wu, Q., Saif, M.: Model-based robust fault diagnosis for satellite control systems using learning and sliding mode approaches. *Journal of computers*, vol. 4, no. 10., pp. 1022–1032. (2009)